Theoretical Studies of Inorganic and Organometallic Reaction Mechanisms. 19. Substitution Reaction in Cyclopentadienyl Metal Dicarbonyls

Hua-Jun Fan and Michael B. Hall*

Department of Chemistry, 3255 TAMU, Texas A&M University, College Station, Texas 77843-3255

Received August 9, 2001

Density functional calculations (B3LYP) of the associative reaction of (η^5-C_5H_4X)$M(CO)_2$ with PR_3 (X = H, Me, Cl; M = Co, Rh, Ir) show that transition-state (TS) effects dominate the reaction rate. Steric factors are less important than electronic ones, unless both the substituents on the cyclopentadienyl (Cp) and the entering ligand are sizable enough to hinder the reaction. Both electron-withdrawing substituents on the Cp ring and electron-donating substituents on the entering ligand facilitate CO substitution. In the associative mechanism, the Cl substituent on Cp lowers the barrier by 3−5 kcal/mol, while the Me substituents on PR_3 lower the barrier by 7−10 kcal/mol. Generally, the ring slipping/folding occurs by lifting two (or three) Cp carbons away from metal by an average value of 0.54 Å, and the two most distant carbons take on more double-bond (C=C) character. For the first time this study identifies the origin of ring slippage and quantifies the degree of ring distortion at the TS by both the M−C bond length changes (ring slip) and C−C−C ring plane angle (ring fold). The calculations show that the Cp ring in the TS has an average folding angle of 12° and slips toward a coordination mode between η^3 and η^2. A single ring substituent takes one particular position with respect to the entering and leaving ligand. Although these group 9 systems clearly react by an associative mechanism, group 7 systems, such as $CpM(CO)_3$ (M = Mn, Tc, Re), undergo substitution reactions by a dissociative mechanism, with significantly higher barriers. The difference in substitution reaction mechanisms for these two 18 e^- systems ($CpM(CO)_3$ group 7 and $CpM(CO)_2$ group 9) arises from several factors: (1) the group 7 systems are already six-coordinate and an associative transition state will be more crowded; (2) the group 9 systems are five-coordinate d^8 structures, which can access a low-energy four-coordinate structure with an orbital available for the attacking ligand.

Introduction

In their kinetic study on the nucleophilic substitution reactions of the saturated complex $CpRh(CO)_2$ (Cp = η^5-C_5H_5), Schuster-Woldan and Basolo[1] suggested that this second-order reaction proceeds by a Cp ring slip, which creates a vacant site at the metal center for the entering nucleophile. It is generally believed that the Cp−metal bonding slips from η^5 to η^3 by localizing Cp−M bonding electrons in the Cp ring. Kinetic studies on $CpCo(CO)_2$ and Cp*$Rh(CO)_2$ (Cp* = η^5-C_5Me_5) systems[2] came to similar conclusions. More recent studies have examined substituent effects on the Cp ring and other ligands.[2−5] In addition, the indenyl ligand was found to accelerate the substitution reaction dramatically because the fused benzene ring presumably stabilizes the ring-slippage, the so-called indenyl effect.[3,6−11] On the basis of the results of these studies, Basolo proposed that the rate enhancement in the Cp complexes was mainly a transition-state effect, rather than a ground-state effect.[12] This suggestion is consistent with the observation that ν_{CO} was not affected by modifications on the ring that changed the reaction rate. Several excellent reviews chronicle the development of this topic.[11−15]

While these kinetic studies have thoroughly documented the macroscopic properties of this reaction, efforts to understand the detailed geometric and electronic effects and to find the ring-slipped intermediate have been varied. For example, crystal structures on indenyl complexes such as $[(indenyl)Ir(H)(PPh_3)_2]^+$,[10]

(1) Schuster-Woldan, H. G.; Basolo, F. *J. Am. Chem. Soc.* **1966**, *88*, 1657.
(2) Rerek, M. E.; Basolo, F. *Organometallics* **1983**, *2*, 372.
(3) Rerek, M. E.; Basolo, F. *J. Am. Chem. Soc.* **1984**, *106*, 5908.
(4) Cheong, M.; Basolo, F. *Organometallics* **1988**, *7*, 2041.
(5) Moreno, C.; Macazaga, M. J.; Delgado, S. *Organometallics* **1991**, *10*, 1124.
(6) Hart-Davi, A. J.; Mawby, R. J. *J. Chem. Soc. A* **1969**, 2403.
(7) White, C.; Mawby, R. J. *J. Chem. Soc. A* **1971**, *8*, 940.
(8) Kowaleski, R. M.; Kipp, D. O.; Stanffer, K. J.; Swepston, P. N.; Basolo, F. *Inorg. Chem.* **1985**, *24*, 3750.
(9) Rerek, M. E.; Ji, L. N.; Basolo, F. *J. Chem. Soc., Chem. Commun.* **1983**, 1208.
(10) Faller, J. W.; Crabtree, R. H.; Habib, A. *Organometallics* **1985**, *4*, 929.
(11) Calhorda, M. J.; Veiros, L. F. *Coord. Chem. Rev.* **1999**, *185−186*, 37.
(12) Basolo, F. *Inorg. Chim. Acta* **1981**, *50*, 65.
(13) Basolo, F. *Inorg. Chim. Acta* **1985**, *100*, 33.
(14) O'Connor, J. M.; Casey, C. P. *Chem. Rev.* **1987**, *87*, 307.
(15) Geiger, W. E. *Acc. Chem. Res.* **1995**, *28*, 351.

10.1021/om010732f CCC: $20.00
Publication on Web 11/30/2001

$[(indenyl)Mo(CO)_2R_2]^+$,[11] and $(indenyl)_2V(CO)_2$[16] clearly showed slippage toward an η^3-conformation. However, efforts to synthesize a stable η^3-slipped Cp intermediate have been less successful.[17,20,21] Therefore, Byers and Dahl examined the other factors, such as the distortion of the Cp ring in the ground state.[18] The inductive (σ) and resonance (π) effects of substituents on the Cp ring in $(\eta^5\text{-}C_5H_4X)Rh(CO)_2$ were also investigated by photoelectron spectroscopy.[22] The ionization band splittings, broadenings, and shifts were correlated with changes in the substitution reaction rates.[22]

Previous theoretical studies in this area include an early molecular orbital analysis and several more recent DFT studies on Cp systems[23−25] and on fused rings such as indenyl.[26−28] Veiros studied $CpMn(CO)_3$, $[(Cp)_2Mn(CO)_2]^+$,[25] and other fused-ring systems[27,28] and suggested that the metal size and geometry also contribute to ring folding or planar-ring slippage. He proposed that an increased mixing between a metal orbital and empty Cp π^* orbital facilitates the ring folding. All of these experimental and theoretical studies acknowledge that both electronic and steric factors may affect the substitution reaction. However, these theoretical studies address only the reactant and product geometric changes and none addresses how ring-slippage in these complexes affects the transition-state geometry.

In this study, we use the reaction $(\eta^5\text{-}C_5H_4X)M(CO)_2 + L \rightarrow (\eta^5\text{-}C_5H_4X)M(CO)L + CO$ (X = H, Cl, Me, L = PMe_3, M = Rh) to examine the substitution reaction in the dicarbonyl group 9 system. The geometries and energetics of the reactants, transition states, and products of these reactions are determined and compared with the available experimental results. The reactions with L = PH_3 as entering ligand are used to compare the triad (X = H, M = Co, Rh, Ir; X = Cl, M = Rh). In addition, the substitution reactions of the group 7 triad $(\eta^5\text{-}C_5H_5)M(CO)_3 + PH_3 \rightarrow (\eta^5\text{-}C_5H_5)M(CO)_2(PH_3) + CO$ (M = Mn, Tc, Re) are calculated to examine how these systems differ from the group 9 dicarbonyls.

Computational Details

The geometries involved in this study have been optimized using DFT methods implemented in Gaussian 98,[29] specifically with the Becke[30] three-parameter hybrid exchange functional and the Lee−Yang−Parr correlation function (B3LYP).[31] The transition states (TS) were obtained using a quasi-Newton method,[32] in which the final updated Hessian has only one negative eigenvalue. These TS geometries were also confirmed by separated frequency calculations, which showed only one imaginary frequency.[33] The metal atoms were described by the Hay and Wadt basis set with effective core potentials (ECP);[34] the outer p orbital in the ECP basis set was replaced by an optimized (41) split valence function from Couty and Hall.[35] A 6-31G* basis set was used for all of the C, O, P, Cl, and H atoms.[36,37] All of these calculations were performed at the Supercomputer Facility of Texas A&M University. The basis set superposition error (BSSE) corrections[38] (calculated with a complete counterpoise procedure) were found to be rather small for PH_3 and only moderate in size for CO. For example, the BSSE corrections for the PH_3 weakly associated reactant precursors $CpM(CO)_2$, M = Co, Rh, and Ir are −0.53, −0.04, and −0.16 kcal/mol, respectively, and BSSE corrections for CO weakly associated product precursors are −2.68, −2.24, and −2.01 kcal/mol, respectively. Since these corrections are rather small and relatively constant, the energies reported here are not BSSE corrected and are relative to the precursor states with weakly bound entering (PR_3) and leaving (CO) ligands, respectively.

Scheme 1

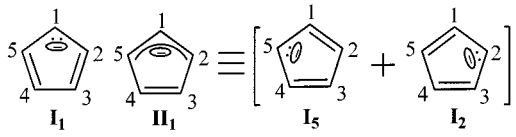

Results and Discussion

A preliminary description of the principal resonance structures of the Cp ring and of distortions of the Cp ring relative to the metal center will be helpful. The five principle resonance structures ($\mathbf{I_{1-5}}$) (Scheme 1) contribute equally when the Cp ring displays equal C(Cp)−C(Cp) bond lengths. However, in a distorted Cp ring, the contributions from these five forms ($\mathbf{I_{1-5}}$) are different. For example, when a single form **I** dominates, one expects two nonadjacent short and three long C−C bond lengths ($\mathbf{I_1}$ in Scheme 1). If two form **I**'s with nonadjacent formal charges dominate (i.e., $\mathbf{I_5}$ and $\mathbf{I_2}$ in Scheme 1), one expects one short, two long, and two intermediate C−C bond lengths ($\mathbf{II_1}$ in Scheme 1). A Cp ring dominated by **II** is sometimes referred to as having "allyl-ene" character.[18]

As discussed in earlier studies, the ideal η^5-Cp ring (A) could be distorted by slipping (B), tipping (C), folding (D), or some combination of these (see Scheme 2). Unless

(16) Kowaleski, R. M.; Rheingold, A. L.; Trogler, W. C.; Basolo, F. *J. Am. Chem. Soc.* **1986**, *108*, 2460.
(17) Simanko, W.; Sapunov, V. N.; Schmid, R.; Kirchner, K.; Wherland, S. *Organometallics* **1998**, *17*, 2391.
(18) Byers, L.; Dahl, L. F. *Inorg. Chem.* **1980**, *19*, 277.
(19) Huttner, G.; Brintzinger, H. H.; Bell, L. G.; Frieddrich, P.; Bejenke, V.; Neugebauer, D. *J. Organomet. Chem.* **1978**, *145*, 329.
(20) Angelici, R. J.; Loewen, W. *Inorg. Chem.* **1967**, *6*, 682.
(21) Casey, C. P.; O'Connor, J. M.; Jones, W. D.; Haller, K. J. *Organometallics* **1983**, *2*, 535.
(22) Lichtenberger, D. L.; Renshaw, S. K.; Basolo, F.; Cheong, M. *Organometallics* **1991**, *10*, 148.
(23) Green, J. C.; Parkin, R. P. G.; Yan, X. F.; Haaland, A.; Scherer, W.; Tafipolsky, M. A. *J. Chem. Soc., Dalton Trans.* **1997**, *18*, 3219.
(24) Arthurs, M.; Piper, C.; Morton-Blake, D. A.; Drew, M. G. B. *J. Organomet. Chem.* **1992**, *429*, 257.
(25) Veiros, L. F. *Organometallics* **2000**, *19*, 5549.
(26) Albright, T. A.; Hofmann, P.; Hoffmann, R.; Lillya, C. P.; Dobosh, P. A. *J. Am. Chem. Soc.* **1983**, *105*, 3396.
(27) Veiros, L. F. *J. Organomet. Chem.* **1999**, *587*, 221.
(28) Veiros, L. F. *Organometallics* **2000**, *19*, 3127.
(29) Frisch, M. J.; Trucks, G. W.; Schlegel, H. B.; Scuseria, G. E.; Robb, M. A.; Cheeseman, J. R.; Zakrzewski, V. G.; Montgomery, J. A., Jr.; Stratmann, R. E.; Burant, J. C.; Dapprich, S.; Millam, J. M.; Daniels, A. D.; Kudin, K. N.; Strain, M. C.; Farkas, O.; Tomasi, J.; Barone, V.; Cossi, M.; Cammi, R.; Mennucci, B.; Pomelli, C.; Adamo, C.; Clifford, S.; Ochterski, J.; Petersson, G. A.; Ayala, P. Y.; Cui, Q.; Morokuma, K.; Malick, D. K.; Rabuck, A. D.; Raghavachari, K.; Foresman, J. B.; Cioslowski, J.; Ortiz, J. V.; Baboul, A. G.; Stefanov, B. B.; Liu, G.; Liashenko, A.; Piskorz, P.; Komaromi, I.; Gomperts, R.; Martin, R. L.; Fox, D. J.; Keith, T.; Al-Laham, M. A.; Peng, C. Y.; Nanayakkara, A.; Gonzalez, C.; Challacombe, M.; Gill, P. M. W.; Johnson, B.; Chen, W.; Wong, M. W.; Andres, J. L.; Gonzalez, C.; Head-Gordon, M.; Replogle, E. S.; Pople, J. A. *GAUSSIAN 98*, Revision A7; Gaussian, Inc.: Pittsburgh, PA, 1998.
(30) Becke, A. D. *J. Chem. Phys.* **1993**, *98*, 5648.
(31) Lee, C.; Yang, W.; Parr, R. G. *Phy. Rev.* **1988**, *B37*, 785.
(32) Schlegel, H. B. *Theor. Chim. Acta* **1984**, *66*, 333.
(33) Foresman, J. B.; Frisch, A. E. *Exploring Chemistry with Electronic Structure Methods*; Gaussian, Inc.: Pittsburgh, PA, 1993.
(34) Hay, P. J.; Wadt, W. R. *J. Chem. Phys.* **1985**, *82*, 299.
(35) Couty, M.; Hall, M. B. *J. Comput. Chem.* **1996**, *17*, 1359.
(36) Hariharan, P. C.; Pople, J. A. *Theor. Chim. Acta* **1973**, *28*, 213.
(37) Francl, M. M.; Pietro, W. J.; Hehre, W. J.; Binkley, J. S.; Gordon, M. S.; DeFrees, D. J.; Pople, J. A. *J. Chem. Phys.* **1982**, *77*, 3654.
(38) Boys, S. F.; Bernardi, F. *Mol. Phys.* **1970**, *19*, 553.

Table 1. Calculated Bond Lengths for the Reaction of $(\eta^5\text{-}C_5H_4X)M(CO)_2$ Complexes with PR_3

$(\eta^5\text{-}C_5H_4X)M(CO)_2 + PMe_3$

	X = H			X = Cl[a]			X = Cl[b]			X = Me[a]			X = Me[b]		
	react.	TS **1**	prod.	react.	TS **2**	prod.	react.	TS **3**	prod.	react.	TS **4**	prod.	react.	TS **5**	prod.
C1−C2	1.427	1.432	1.409	1.448	1.451	1.446	1.453	1.459	1.447	1.458	1.465	1.454	1.458	1.473	1.454
C2−C3	1.448	1.473	1.450	1.402	1.373	1.422	1.419	1.399	1.419	1.417	1.367	1.417	1.420	1.398	1.419
C3−C4	1.402	1.368	1.407	1.450	1.467	1.423	1.426	1.432	1.426	1.429	1.473	1.428	1.425	1.432	1.425
C4−C5	1.452	1.461	1.438	1.422	1.435	1.448	1.451	1.470	1.446	1.446	1.435	1.442	1.449	1.475	1.445
C5−C1	1.418	1.399	1.436	1.422	1.396	1.398	1.397	1.365	1.399	1.406	1.400	1.409	1.404	1.367	1.406
M−C1	2.358	2.374	2.381	2.327	2.821	2.434	2.42	3.056	2.428	2.392	2.809	2.394	2.402	3.078	2.402
M−C2	2.291	2.334	2.371	2.394	3.105	2.330	2.315	2.683	2.335	2.310	3.122	2.327	2.300	2.664	2.315
M−C3	2.38	2.916	2.377	2.364	2.829	2.361	2.342	2.368	2.358	2.347	2.881	2.371	2.344	2.354	2.363
M−C4	2.374	3.088	2.386	2.290	2.286	2.317	2.281	2.348	2.308	2.278	2.290	2.305	2.281	2.334	2.306
M−C5	2.310	2.712	2.292	2.378	2.433	2.442	2.419	2.922	2.442	2.385	2.396	2.399	2.387	2.926	2.405
M−C(CO)	1.880	2.095	4.143	1.888	1.875	1.847	1.886	1.868	1.848	1.879	1.876	1.846	1.883	1.871	1.846
M−C(CO)	1.879	1.870	1.841	1.876	2.207	3.881	1.877	2.114	3.775	1.881	2.135	3.821	1.879	2.082	3.872
M−P	5.062	2.314	2.284	5.087	2.287	2.281	5.074	2.311	2.280	5.227	2.299	2.281	5.049	2.323	2.282

$(\eta^5\text{-}C_5H_4X)M(CO)_2 + PH_3$

(X, M)	X = H, M = Co			X = H, M = Rh			X = H, M = Ir			X = Cl, M = Rh[b]			X = H, M = Mn		
	react.	TS 6	prod.	react.	TS 7	prod.	react.	TS 8	prod.	react.	TS 9	prod.	react.	TS 10	prod.
C1−C2	1.420	1.372	1.410	1.422	1.367	1.420	1.428	1.466	1.434	1.453	1.475	1.412	1.417	1.421	1.426
C2−C3	1.446	1.464	1.435	1.450	1.47	1.424	1.446	1.431	1.448	1.413	1.424	1.450	1.432	1.428	1.419
C3−C4	1.406	1.422	1.437	1.401	1.424	1.448	1.411	1.435	1.411	1.433	1.411	1.402	1.422	1.413	1.433
C4−C5	1.444	1.416	1.409	1.450	1.421	1.401	1.446	1.471	1.448	1.445	1.467	1.448	1.424	1.414	1.420
C5−C1	1.423	1.464	1.447	1.423	1.473	1.453	1.428	1.368	1.422	1.400	1.362	1.430	1.431	1.428	1.429
M−C1	2.163	2.603	2.151	2.359	2.836	2.293	2.364	2.917	2.350	2.407	2.887	2.386	2.183	2.275	2.185
M−C2	2.114	2.574	2.164	2.304	2.811	2.363	2.290	2.356	2.271	2.338	2.364	2.353	2.183	2.275	2.196
M−C3	2.163	2.16	2.082	2.385	2.323	2.314	2.350	2.191	2.353	2.348	2.304	2.404	2.182	2.653	2.189
M−C4	2.166	2.113	2.158	2.384	2.236	2.401	2.326	2.353	2.377	2.274	2.499	2.371	2.185	2.922	2.165
M−C5	2.109	2.223	2.153	2.301	2.367	2.370	2.353	2.917	2.332	2.415	2.954	2.274	2.181	2.653	2.165
M−C(CO)	1.749	1.748	1.730	1.881	1.865	1.854	1.857	1.854	1.837	1.877	1.866	1.850	1.794	1.792	1.782
M−C(CO)	1.748	2.041	3.600	1.880	2.244	3.752	1.863	2.317	3.900	1.888	2.156	3.975	1.794	2.443	4.271
M−P	5.075	2.277	2.159	5.894	2.419	2.268	5.125	2.300	2.250	4.540	2.327	2.273	5.345	2.287	2.233

[a] Opposite-side pathway, [b] Same-side pathway.

Scheme 2

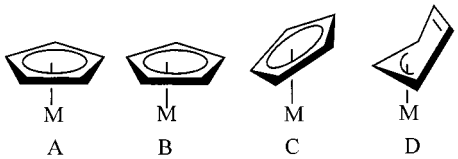

the rest of the metal fragment provides a rotational axis of high symmetry, such as the C_3 of $M(CO)_3$, it will be difficult to make a clear distinction (from the M−C(Cp) distances alone) among slipping (B), tipping (C), and folding (D). Therefore, we will use differences in the M−C(Cp) distance as a measure of the slipping and tipping and will refer to these distortions as "slipping". We will then define folding with respect to the carbon atoms alone by defining one plane consisting of the three carbons with the shortest M−C(Cp) distance and another consisting of the three carbons with the longest M−C(Cp) distance. The angle between these two planes will define the folding angle of the Cp ring.

Substitution Reactions of $(\eta^5\text{-}C_5H_5)Rh(CO)_2$ with PMe_3. A selection of optimized bond lengths of reactants, transition states, and products are listed in Table 1 (all reactants and product structures listed in Table 1 are precursor states with weakly bound entering (PR_3) and leaving (CO) ligands, respectively). The corresponding TS structures with selected bond lengths are shown in Figure 1. The $CpRh(CO)_2$ reactant shows two nonadjacent longer C−C bonds of 1.45 Å linking three somewhat shorter C−C bonds of 1.40, 1.42, and 1.43 Å. Although the differences between these C−C(Cp) bond lengths are small, they indicate that the Cp ring already has some "allyl-ene" character,[18] i.e. a slight preference for $\mathbf{II_1}$. The shortest, and presumably strongest, Rh−C(Cp) bonds are between the terminal allyl-carbons (C2 and C5) and the metal (2.29 and 2.31 Å), while the other three M−C(Cp) bond lengths are about 0.09 Å longer. Nevertheless, it is reasonable to consider that this Cp ring is still η^5-bonded to Rh and the ring is folded only by 4.2°. These calculated C−C and Rh−C(Cp) bond lengths are comparable to the crystal structure values measured for $Cp^*Rh(CO)_2$,[42,43] which shows similar bond length patterns. The slightly different Rh−C(Cp) and C−C bond lengths can be attributed to the location of the carbonyl ligands relative to the Cp ring. The primary effect of the carbonyl locations in the equilibrium structure is to orient the only strongly σ-bonding d orbital toward C2 and C5. In addition, the strong back-bonding of the carbonyls withdraws more electron density from the metal and enhances the bonding between the metal d_π orbitals and Cp ring p_π orbitals.[44,45]

The optimized geometry of the transition state (**1**) for the reaction $CpRh(CO)_2 + PMe_3 \rightarrow CpRh(CO)PMe_3 + CO$ is shown in Figure 1. This TS structure reveals a late TS with the Rh−CO(leaving) bond length 0.21 Å

(39) Loushin, S. K.; Liu, S.; Dykstra, C. E. *J. Chem. Phys.* **1986**, *84*, 2720.
(40) Fischer, E. O.; Brenner, K. S. *Naturforsch.* **1962**, *17B*, 774.
(41) King, R. B.; Bisnette, M. B. *J. Organomet. Chem.* **1967**, *8*, 287.
(42) Lichtenberger, D. L.; Blevins, C. H., II; Ortega, R. B. *Organometallics* **1984**, *3*, 1614.
(43) Braunstein, P.; Lehner, H.; Matt, D.; Tiripicchio, A.; Camellini, M. T. *New J. Chem.* **1985**, *9*, 597.
(44) Chinn, J. W.; Hall, M. B. *J. Am. Chem. Soc.* **1983**, *105*, 4930.
(45) Low, A. A.; Hall, M. B. *Int. J. Quantum Chem.* **2000**, *77*, 152.

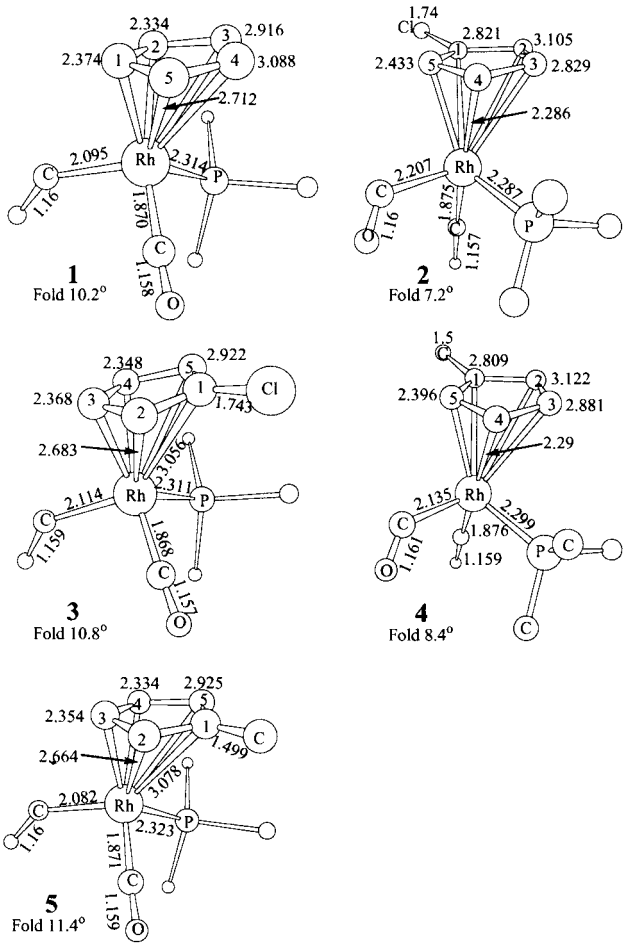

Figure 1. DFT optimized geometries (Å) of transition states for the CO substitution reaction of (η^5-C_5H_4X)Rh-$(CO)_2$ with PMe_3 (**1**: X = H; **2**: X = Cl, PMe_3 attacks opposite side of Cl; **3**: X = Cl, PMe_3 attacks same side of Cl; **4**: X = Me, PMe_3 attacks opposite side of Me; **5**: X = Me, PMe_3 attacks same side of Me. All H's are omitted for clarity.)

longer than that of the reactant and the Rh−P bond length 0.03 Å longer than that of the product. Compared to the corresponding C−C bonds of the Cp ring in the reactant, the two shortest C−C bonds (C1−C5 and C3−C4) become slightly shorter in the TS (1.40 and 1.37 Å), while two nonadjacent longer C−C bonds (C2−C3 and C4−C5) become slightly longer (1.47 and 1.46 Å). These bond length changes suggest that the Cp gains both resonance form $\mathbf{II_1}$ and resonance form $\mathbf{I_2}$ character. Combination of these two resonance forms is responsible for the different C1−C5 and C1−C2 bond lengths as observed here for TS **1**. In addition, the greater Rh−C(Cp) bond length differences are found at the TS. Two carbons (C1 and C2) retain fairly short Rh−C bond lengths (2.33 and 2.37 Å), while the other three carbons show increases of 0.54 (C3), 0.71 (C4), and 0.40 Å (C5). Correspondingly, the two carbons with the longest Rh−C bonds (C3 and C4) have the shortest C−C bond (1.37 Å), a length that indicates nearly double-bond character. The pattern of C−C and Rh−C bond lengths is consistent with the mixture of resonance forms $\mathbf{II_1}$ and $\mathbf{I_2}$ mentioned above. In addition to the different bond lengths between C1−C2 and C1−C5, these two resonance forms ($\mathbf{II_1}$ and $\mathbf{I_2}$) also account for the intermediate Rh−C5 bond length. This same pattern

Scheme 3

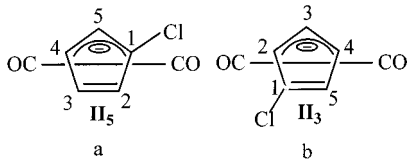

will be seen in the other TS. The Cp folding angle for TS **1** is 10.2°, a net increase of 5.9° from that of the reactant.

Substitution Effect on the Cp Ring. Previous kinetic studies examined the reaction rate dependence on the Cp ring substitution with both Cl and Me substituents.[1−4] Photoelectron spectroscopy[22] also examined the electronic effect of these substitutions. A Cl substituent is σ electron-withdrawing, but the lone pair of Cl can π-donate to the empty π^* orbitals on the Cp ring. Therefore, the ability of Cl to influence the electron flow between the Cp ring and the metal will depend on the balance of these two factors. On the other hand, Me is mainly σ electron-donating. Since an attacking nucleophile will add electron density to the metal center, a more electron-withdrawing substitution on the Cp ring should stabilize the transition state and show faster reaction rates.[1−4] The experimental studies showed a slightly slower reaction rate of the Me substituent and much faster reaction rate with the Cl substituent compared with unsubstituted Cp ring. These results suggest that the difference in σ-bonding between the substituent (Me and Cl) and the Cp ring dominates the reaction rate. In the following, we will examine the geometric changes arising from the Cl substituent and methyl substituent, while hints of a larger π resonance effect for Cl are seen.

Cl-Substitution on the Cp Ring. Previous photoelectron spectroscopy[22] suggested that the Cl substituent on the Cp ring has an orientation neither perpendicular nor parallel to the $Rh(CO)_2$ plane. Indeed, our calculations show that this substituted ring prefers intermediate orientations as shown in Scheme 3. Like the $CpRh(CO)_2$ reactant, the Cp ring structure of the Cl-substituted reactant also shows "allyl-ene" character. Both of the rotamers shown in Scheme 3 were found to be minima. One has the Cl substituent bound to a terminal allyl-carbon (Scheme 3a), and the other has it bound to an ene-carbon (Scheme 3b). The optimized C−C bond lengths of both rotamers show a slight preference for the **II** resonance form, as shown in Scheme 3, which reflects the same bond pattern and similar C−C bond lengths as those in the $CpRh(CO)_2$ reactant. The Rh−C(Cp) bonds also show a similar pattern. Furthermore, these two rotamers (the only two minima for the reactant) differ only by 0.04 kcal/mol. Thus, the pattern of C−C and Rh−C bond lengths is set by the ring's relative position with the CO bonds and is only weakly affected by the substitution.[44,45] The Cp ring folding angles for both reactants are 2.5° and 5.0° for a and b in Scheme 3, respectively, a value similar to that in the unsubstituted reactant. Overall, the substituent on the Cp ring has little impact on the reactant geometrically.

In these intermediate orientations (Scheme 3), the PMe_3 can approach either from the same or from the

opposite side of the substituted carbon. In our TS optimization, a in Scheme 3 was used as the reactant for the opposite-side pathway and b in Scheme 3 was used as the reactant for the same-side pathway. The TS structures for the opposite-side pathway (TS **2**) and same-side pathway (TS **3**) are shown in Figure 1, and selected geometric parameters of the reactants, TSs, and products are listed in Table 1. Like TS **1** for the reaction with the unsubstituted Cp complex, TS **2** for the opposite-side pathway reveals both dramatic Rh−C(Cp) and significant C−C bond length changes. For example, the C−C bond lengths of the Cp ring indicate an increase in the contribution of the $\mathbf{I_4}$ and $\mathbf{II_5}$ resonance forms in TS **2** (compared to excess $\mathbf{II_5}$ resonance form of **a** in Scheme 3). As shown in the unsubstituted CpRh-$(CO)_2$ case, we demonstrated that the shortest C−C bond (the C's with the longest Rh−C bonds) lifts to accommodate the entering ligand. Here, we observe the same lift pattern. As a result, C1, C2, and C3 now have the longest Rh−C(Cp) bonds in TS **2**. Their bond lengths show net increases of 0.49, 0.71, and 0.47 Å, respectively, from those of reactant a in Scheme 3. The amount of Rh−C bond length increases are similar to those of TS **1** and are consistent with increase in resonance forms of $\mathbf{II_5}$ and $\mathbf{I_4}$. As a result of these geometric changes, the Cp ring is η^2-bond to the Rh center via C4 and C5, with Rh−C4 being the shortest Rh−C bond. The Cp ring-folding angle for TS **2** is 7.2°, a net increase of 4.7° from that of reactant a in Scheme 3.

The geometric changes of TS **3** are similar to those of TS **2**. For example, TS **3** reflects an increase in both resonance forms $\mathbf{I_4}$ and $\mathbf{II_3}$, while the Cp ring in the reactant (Scheme 3b) begins with only a slight excess of resonance form $\mathbf{II_3}$. The Rh−C(Cp) distances also show two short Rh−C bonds (C3 and C4), one intermediate Rh−C bond (C2), and two long Rh−C bond lengths (C1 and C5), which suggest the Cp is essentially η^2-bond to Rh via C3 and C4. The three longest Rh−C(Cp) bonds show the greatest increases: 0.64 (C1), 0.37 (C2), and 0.50 Å (C5). This result is consistent with increases in resonance forms $\mathbf{II_3}$ and $\mathbf{I_4}$. As a result of these geometric changes, the Cp ring now has a folding angle of 10.8°, an increase of 5.8° from that of reactant b in Scheme 3. The normal mode of the single imaginary frequency from separate frequency calculations of both TSs (**2** and **3**) shows Rh−CO bond breaking (forming) and Rh−P bond forming (breaking). We will discuss the Cl substituent's effect on the reaction rate in more detail later.

Me-Substitution on the Cp Ring. Like the reactions for the system with the Cl substituent, two TSs for the reaction with a methyl-substituted Cp ring are found and the optimized structures are shown in Figure 1 (opposite-side TS **4** and same-side TS **5**). The selected geometric parameters of reactants, TSs, and products are listed in Table 1. Both Me-substituted reactants have only a small energy difference (0.04 kcal/mol) and folding angles of 4.5° and 4.6°, compared to 4.3° for the unsubstituted reactant. Despite the different reaction rates for the reactions with the Cl- and Me-substituted Cp rings, there are many similarities in the structures of reactants. For example, the MeCp ring of both reactants has excess $\mathbf{II_3}$ resonance character, and the Rh−C(Cp) bond pattern is much like the Cl-substituted reactant. However, close examination of the bond lengths found that the Me-substituted reactant has geometric parameters more like those of the unsubstituted reactant than those of the Cl-substituted reactant. One possible explanation could be the difference in the π-interactions between the Me and the Cp ring, compared to those between the Cl and the Cp ring.

Scheme 4

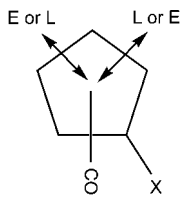

Interestingly, the geometric changes for the Me-substituted TSs are also similar to those of both the unsubstituted and Cl-substituted complexes. Like the other TSs, the Me-substituted TSs show additional contributions from $\mathbf{I_4}$ and $\mathbf{II_5}$ for the opposite-side pathways (TS **4**) and $\mathbf{I_4}$ and $\mathbf{II_3}$ for the same-side pathway (TS **5**). Furthermore, these TSs show that the Cp is η^2-bonded to the Rh center, with TS **5**'s two shortest Rh−C bond lengths being more equal than those in TS **4**. The other three remaining carbons have much longer Rh−C(Cp) bonds, and the increases relative to the corresponding reactants are 0.81, 0.53, and 0.42 Å for TS **4** and 0.68, 0.54, and 0.36 Å for TS **5**. The folding angles are found to be 8.4° and 11.4° for TS **4** and **5**, respectively. In support of a difference in the π interaction between the Me and Cl substituents, the calculations predict that the Cl−C1 bond length shortens by about 0.006 Å in the transition states. Although this change is small, it is consistent with increasing π resonance effects in the transition state. The Me−C1 bond length shows a shortening in the TS whose magnitude is about half of that of the Cl.

Despite the different substituents on the Cp ring and the different directions available for the entering nucleophile, these four TSs (**2**−**5**) have the unified structure illustrated in Scheme 4, in which the only difference is the relative position of the entering ligand (E) and the leaving ligand (L). The remaining CO always takes the same location relative to the substituent on the Cp ring. If the entering ligand (E) and the leaving ligand (L) were the same, the opposite- and same-side TSs would be identical. Since E and L are different in this study, we are able to locate two different TSs corresponding to the different positions of the nucleophiles.

Overall, the Rh−C(Cp) changes and Cp folding angles among TSs **1** to **5** introduced by the attack of PMe_3 are similar. The two carbons with the longest Rh−C lengths always have the shortest C−C bond, and the Cp ring is η^2-bonded to the metal center. Furthermore, our calculated CO stretching frequencies for these reactants also indicate only small changes of 5−10 cm^{-1} upon substitution (see Table 2), in agreement with experimental observations. Again, the similarity of the reactant structures and calculated CO stretching frequencies suggests that differences in the reaction rate are controlled by transition-state effects, rather than ground-state effects.

Table 2. Comparison between the Calculated CO Stretching Frequencies (B3LYP) and Experimental Values[4,40]

reactant	calculated		experiment	
(η^5-C_5H_4Cl)Rh(CO)$_2$	2072	2126	1991	2053
(η^5-C_5H_4Me)Rh(CO)$_2$	2056	2115	1978	2041
CpCo(CO)$_2$	2073	2118	1965	2037
CpRh(CO)$_2$	2066	2120	1987	2051
CpIr(CO)$_2$	2061	2019	1957	2057
CpRh(CO)PMe$_3$	2034		1957	
(η^5-C_5H_4Cl)Rh(CO)PMe$_3$	2048		1963	
(η^5-C_5H_4Me)Rh(CO)PMe$_3$	2036		1950	

Calculated Potential Energy Surface. The calculated thermodynamic parameters for the reaction (η^5-C_5H_4X)Rh(CO)$_2$ + PMe$_3$ → (η^5-C_5H_4X)Rh(CO)(PMe$_3$) + CO (X = H, Cl, Me) are summarized in Table 3. Our calculated $\Delta H^{\ddagger}$ for unsubstituted Cp reaction with PMe$_3$ is 17.7 kcal/mol. This value is close to the measured values of 15 kcal/mol for CpRh(CO)$_2$ with either PEt$_2$-Ph or P(*n*-OC$_4$H$_9$)$_3$,[1,4] 15.6 ± 2.0 kcal/mol for the (MeCp)-Rh(CO)$_2$ with PPh$_3$,[4] and 13.6 kcal/mol for (Cp*)RhCO$_2$ with P(OEt)$_3$.[2] The predicted $\Delta H^{\ddagger}$ of the Cl-substituted reaction for the opposite- and same-side approach of the PMe$_3$ ligand are 3.1 and 4.3 kcal/mol lower than that for the unsubstituted Cp. These predictions are in agreement with the experiment which shows a faster reaction rate for (η^5-C_5H_4Cl)Rh(CO)$_2$ than for (Cp)Rh-(CO)$_2$. Our calculated value for the reaction between (η^5-C_5H_4Me)RhCO$_2$ and PMe$_3$ is 16.9 kcal/mol. The calculated difference, Cp vs (C_5H_4Me) complex, is within the experimental error of these differences. Our calculations also predict that the substitution reactions are endothermic, with $\Delta H°$ of 4.2 (Cp), 4.0 (Me-substituted), and 2.7 kcal/mol (Cl-substituted). Since the $\Delta G°$ values are also slightly positive, one may conclude that the reaction is driven to completion by the CO release.

The Co, Rh, and Ir Triad. In this section, PH$_3$ is used as the entering ligand to study the substitution reaction of CpM(CO)$_2$, where M = Co, Rh, and Ir. As a comparison, the Cl-substituted reactant with PH$_3$ is also presented. One should keep in mind that there are two major differences when PH$_3$ is the attacking ligand: first it is smaller than other phosphines and second, and more important, it is a poorer electron donor. Experimental study showed that the size of the entering ligand does affect the reaction rate.[2] For example, Cp*Rh(CO)$_2$ reacts with the PMe$_3$, which has a cone angle of 118°, while the PPh$_3$ ligand, which has a larger cone angle of 145°, shuts down the reaction.[2] Differences in the electron-donating ability of the entering ligand also affect the reaction as the $\Delta H^{\ddagger}$ of the Cp*Co(CO)$_2$ reactant increases from 15.8 to 18.2 kcal/mol, when the entering ligand changes from P(*n*-Bu)$_3$ to P(OEt)$_3$.[2] Although PH$_3$ is rarely used as a ligand, the calculated trend from the reaction of the triad should provide some useful comparison of the metals and the electronic effect of a poor entering ligand.

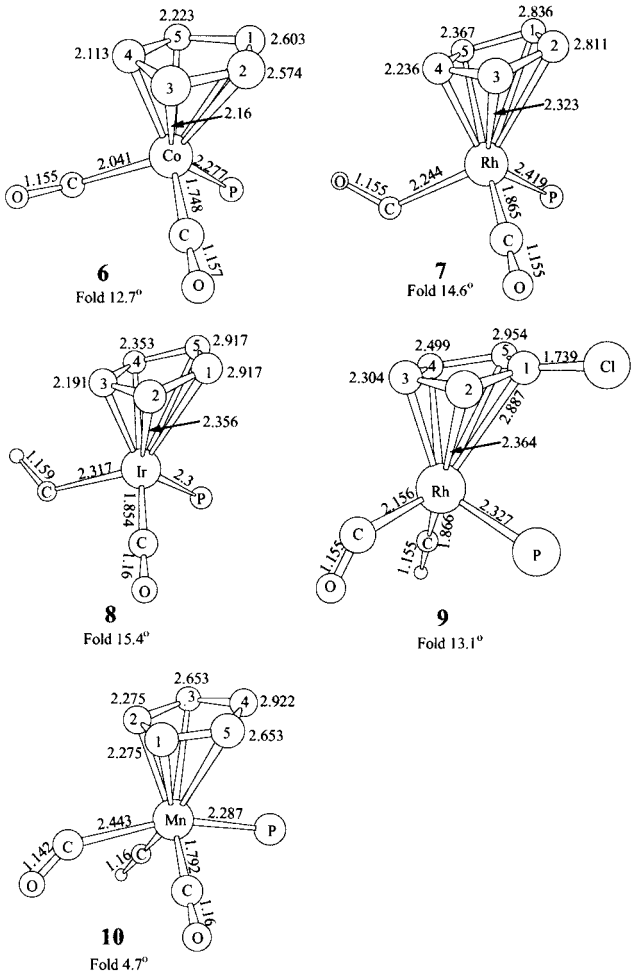

Figure 2. DFT optimized geometries (Å) of transition states for the CO substitution reaction of (η^5-C_5H_4X)M(CO)$_2$ with PH$_3$ (**6**: X = H, M = Co; **7**: X = H, M = Rh; **8**: X = H, M = Ir; **9**: X = Cl, M = Rh PH$_3$ attacks same side of Cl) and TS **10** for the assumed associative reaction pathway for CO substitution reaction of CpMn(CO)$_3$ with PH$_3$. (All H's are omitted for clarity.)

The TSs involving CpCo(CO)$_2$ (**6**), CpRh(CO)$_2$ (**7**), and CpIr(CO)$_2$ (**8**) with PH$_3$ are shown in Figure 2, and the

Table 3. Energies for the Reaction (η^5-C_5H_4X)M(CO)$_2$ + L → (η^5-C_5H_4X)M(CO)(L) + CO (X = H, Cl, Me, M = Co, Rh, Ir)

X	$\Delta E^{\ddagger c}$	$\Delta E^{\ddagger c}_{ZPE}$	$\Delta H^{\ddagger c}$	$\Delta S^{\ddagger d}$	$\Delta G^{\ddagger c}$	$\Delta E°^{c}$	$\Delta E°^{c}_{ZPE}$	$\Delta H°^{c}$	$\Delta S°^{d}$	$\Delta G°^{c}$
Reaction with M = Rh, L = PMe$_3$ Ligand										
H	18.9	18.1	17.7	13.2	21.7	4.63	3.67	4.24	−5.4	2.63
Cl[a]	15.8	15.0	14.6	14.3	18.9	2.97	2.35	2.75	1.6	3.23
Cl[b]	14.5	13.9	13.4	12.7	17.2	2.93	2.20	2.64	−3.4	1.63
Me[a]	18.8	17.8	17.4	13.4	21.4	4.80	4.06	4.45	2.2	5.09
Me[b]	18.3	17.3	16.9	10.6	20.1	4.64	3.61	3.61	2.2	4.26
Reaction with L = PH$_3$ Ligand										
H, Co	30.9	30.4	29.7	14.4	34.0	16.2	16.3	16.2	3.35	17.2
H, Rh	28.3	27.7	27.1	13.1	31.0	12.0	12.3	12.1	5.03	13.6
H, Ir	34.4	34.3	33.5	16.1	38.3	17.5	17.8	17.6	3.35	18.6
Cl,[b] Rh	21.8	21.9	21.1	15.4	25.7	10.4	10.3	9.8	5.70	11.5

[a] Opposite-side pathway. [b] Same-side pathway. [c] kcal·mol^{-1}. [d] cal·mol^{-1}·deg^{-1}.

selected bond lengths for the reactants, TSs, and products are listed in Table 1. The slight differences in the geometries of the Rh reactants (PMe_3 vs PH_3) are due to the presence of the entering ligand in the precursor listed in Table 1. Compared to Rh, the Cp ring conformations of the reactant for the other metals (Co and Ir) also show an excess of the **II$_1$** resonance form with similar small Cp folding angles (Co: 3.3° and Ir: 3.2°). However, the Cp rings of the TSs show stronger dominance of a **II** resonance form, rather than a mixture of **I** and **II**, as shown above with PMe_3 as entering ligand. Furthermore, judging from the M−C(Cp) bond lengths, the Cp is η^3-bonded and only two of the M−C(Cp) bonds are lengthened. At the TSs, the Cp folding angles are 12.7° (Co), 14.8° (Rh), and 16.2° (Ir), which are larger than any of the ones with the PMe_3 ligand. However, the increases of the Rh−C(Cp) distances from reactant to TS are comparable to those for TS **2**−**5** with PMe_3 as the entering ligand. The larger folding angles of the Cp ring and similar Rh−C(Cp) increases at the TS are somewhat surprising considering the smaller size of the PH_3 ligand. Apparently, the size of entering ligand has little effect on the Cp ring's folding angle, which is influenced by the metal.

The calculated $\Delta H^{\ddagger}$ values for the substitution reaction with PH_3 are 29.7, 27.1, and 33.5 kcal/mol for Co, Rh, and Ir, respectively. The value for the Rh complex with PH_3 is much larger than that calculated for Rh with PMe_3 (barrier for TS **1** is 17.7 kcal/mol). These larger activation barriers can be attributed to the poorer σ-donating ability of the PH_3 ligand, compared with PMe_3. Furthermore, the irregularity of trend in the triad has been seen in other studies and suggests that the Rh−C(Cp) bond is the weakest in this triad.[1,12]

Cl-Substituent Effect with PH_3. As a further check of the calculated trends, we examined the reaction between the PH_3 and the Cl-substituted reactant along the same-side pathway (TS **9**) and compared the results with reaction using the PMe_3 ligand (TS **3**). The structure of TS **9** is shown in Figure 2, and the geometric parameters for reactant, TS, and product are listed in Table 1. Again, we observe an excess **II$_3$** resonance character for the reactant. Like the TS for the other reactions with the PH_3 ligand, the Rh−C(Cp) bond lengths suggest that the Cp ring is η^3-bonded with the metal and only two of Rh−C bonds (C1 and C5) show large increases (0.48 and 0.54 Å, respectively) on reaching TS **9**. The calculated Cp folding angle for TS **9** is 13.1°, a net increase of 8.7° from the reactant. The calculated $\Delta H^{\ddagger}$ value for TS **9** is 21.1 kcal/mol, which is 7.7 kcal/mol greater than that for TS **3**. This increase in $\Delta H^{\ddagger}$ is consistent with the differences calculated for $CpRh(CO)_2$ with PMe_3 and PH_3 (TS **1** and TS **7**). Furthermore, the decrease in $\Delta H^{\ddagger}$ when adding a Cl substituent to the ring ($CpRh(CO)_2$ to (η^5-C_5H_4Cl)$Rh(CO)_2$) is also consistent with that for PMe_3. Again, electron-withdrawing substitution on the ring and stronger donor ligands lead to lower reaction barriers.

Reaction of $CpM(CO)_3$, M = Mn, Tc, Re. Similar calculations on the group 7 triad show that a dissociative pathway is preferred. As a representative of the triad, the structure of the associative TS of $CpMn(CO)_3$ **10** is shown in Figure 2, and the selected bond lengths for this associative reaction are shown in Table 1. Importantly, the calculated energy required to dissociate one CO in $CpMn(CO)_3$ (52.7 kcal/mol) is lower than the TS energy on the assumed associative reaction pathway (56.3 kcal/mol). Thus, in agreement with experiment, we predict that the $CpMn(CO)_3$ reaction proceeds by an dissociative mechanism, not an associative one.[20] Interestingly, the TS structure found for the assumed associative mechanism for the $CpMn(CO)_3$ reaction with the PH_3 ligand shows that the ring is slipped and tipped with little folding (4.7°) compared to those of the group 9 triad. Other studies have found similar results.[25] This difference in the reaction mechanisms of these two 18 e^- species can be attributed to the following factors. First, the group 7 system is six-coordinate, while the group 9 system is five-coordinate, and thus, the group 7 reactant is more crowded than the group 9 reactant. Second, as discussed earlier, the reactants of group 9 already show Cp ring distortion. This distortion is consistent with the d^8 metal, which has a tendency for a square planar geometry. Both these factors favor the group 9 system preferring an associative reaction mechanism and group 7 preferring a dissociative mechanism.

Conclusions

All of the TSs obtained in this study suggest that the Cp ring is slipped and tipped toward η^2- or η^3-bonding with the metal. The average lengthening of M−C(Cp) from reactant to TS is 0.54 Å. The principal Cp ring resonance structures for the TS vary from mainly form **II** with an η^3-Cp ligand when PH_3 is the entering ligand to a mixture of forms **II** and **I** with an η^2-Cp ligand when PMe_3 is the entering ligand. The amount of the Cp ring folding varies from a net increase of 4° to 13° from reactant to TS. No direct relationship was found between the entering ligand size and the folding angle. However, a consistent increase in the folding angles was observed on changing the metal from Co to Ir. Furthermore, the electronic properties of the entering ligand and the substituents on the Cp ring have greater impact on the reaction barrier than their size unless the species are so bulky that they no longer react. For example, a σ-withdrawing substituent such as Cl on the Cp ring lowers the reaction barrier 3−5 kal/mol and a stronger σ donor as the entering ligand, PMe_3, lowers the barrier 7−10 kcal/mol compared to those with PH_3. For the TS of monosubstituted Cp ring system (C_5H_4X)M(CO)(E)(L), the entering (E) and leaving (L) ligand position themselves with respect to the X substituent such that X nearly eclipses the remaining CO ligand. In agreement with experiment, our calculations show that the five-coordinate d^8 group 9 dicarbonyls, $CpM(CO)_2$, which have access to a four-coordinate geometry, undergo associative substitution reactions, while the six-coordinate d^6 group 7 tricarbonyls, $CpM(CO)_3$, which are coordination saturated, undergo dissociative substitution reactions.

Acknowledgment. We gratefully acknowledge the National Science Foundation (Grant No. CHE 9800184) and The Welch Foundation (Grant No. A-648) for financial support of this work.

OM010732F